Virchows Arch [Pathol Anat] (1984) 402:209–237

Virchows Archiv A

Ultrastructural analysis of human proximal tubules and cortical interstitium in chronic renal disease (Hydronephrosis)*

Jens Chr. Møller[1,2], Elisabeth Skriver[1], Steen Olsen[2], and Arvid B. Maunsbach[1]

[1] Department of Cell Biology, Institute of Anatomy, University of Aarhus
[2] University Institute of Pathology, Kommunehospitalet, DK 8000 Aarhus, Denmark

Summary. A systematic ultrastructural analysis of proximal tubule atrophy and cortical interstitial changes was carried out in human chronic nephropathy. The investigation was based on human hydronephrotic kidneys, which had been surgically removed and subsequently perfusion-fixed for light and electron microscopy. Normal kidney tissue, which was derived from nephrectomy specimens with pathological changes confined to part of the kidney or to the renal pelvis, was used for control material. A slight degree of proximal tubule atrophy was characterized by reduction of mitochondria and basolateral membranes, enlargement of large endocytic vacuoles and increased numbers of lysosomes containing lamellar material. In moderate atrophy these changes were further accentuated, and in addition there was an increasing loss of microvilli and a reduction of endocytic invaginations and small endocytic vacuoles. In severe atrophy all types of organelles were sparse and the architecture of the tubule cells greatly simplified. A distinctive feature of atrophic tubules was the presence in the tubule cells of large bundles of actin-like filaments, which were often associated with outpouchings of basal cell parts and basement membrane. The reduction of mitochondria and basolateral cell membranes and the changes of endocytic vacuoles and lysosomes indicate that proximal tubule atrophy also in early stages may be associated with impairment of tubular transport processes. Comparisons with previous observations in various types of experimentally induced tubule cell degeneration and with the ultrastructure of regenerating proximal tubule cells provide some evidence that degenerative changes as well as imperfect regeneration of tubule cells may contribute to the alterations of ultrastructure in tubular atrophy. It is suggested that changes of the cortical interstitium may be of pathogenic importance

* This work was supported by grants from the Danish Medical Research Council (no 12-0528) and from the Research Foundation at the University of Aarhus.

Offprint requests to: J.Chr Møller at the above address

for the progression of tubular atrophy by altering the spatial relationships between tubules and capillaries.

Key words: Proximal tubule – Atrophy – Cortical interstitium – Human nephropathy – Ultrastructure

Tubular atrophy and cortical interstitial fibrosis (tubulo-interstitial disease) are common markers of advanced chronic renal disease regardless of the underlying cause. However, in its light microscopic sense the term "tubular atrophy" is not a well defined entity. It is generally applied to tubules of reduced size and having thickened basement membranes, but entails little or no information concerning structural alterations at the cellular or subcellular level, which may be crucial for the evaluation of changes in tubular functions. Furthermore, the pathogenic mechanisms underlying tubular atrophy remain to be clarified.

The need for a more detailed knowledge of tubulo-interstitial disease has been stressed by results of structure-function analyses in human chronic renal disease. Thus, it has been amply demonstrated that in several types of chronic nephropathy the decrease of glomerular filtration rate (as expressed by the level of serum creatinine or the creatinine clearence) is quantitatively well correlated with the degree of tubular damage (atrophy) or with the increase in cortical interstitium, whereas there appears to be no correlation between the glomerular filtration rate and type or degree of glomerular disease (Bohle et al. 1977a and b; Grund et al. 1978; Jepsen and Mortensen 1979; Mackensen et al. 1979; Mackensen-Haen et al. 1981; Riemenschneider et al. 1980; Risdon et al. 1968; Schainuck et al. 1970; Sloper et al. 1980). Similar observations have been made in lithium-induced chronic nephropathy in rats (Ottosen PD, Christensen S, Sigh B, Olsen S, personal communication. It therefore appears likely that tubulo-interstitial disease may play a more important role in the pathogenesis of chronic renal insufficiency than previously thought.

The present study was carried out to provide an improved basis for the understanding of the observed structure-function relations in human chronic renal disease by analysing systematically the ultrastructural changes associated with various degrees of proximal tubule atrophy and by relating these to changes in the surrounding interstitium. As a model of human chronic renal disease we have chosen renal parenchymal atrophy associated with non-infected hydronephrosis. The reasons for this choice were: 1) that it is a well defined pathological entity; 2) that it exhibits a great range of tubular and interstitial alterations and 3) that nephrectomy specimens were available in sufficient numbers. The basic ultrastructural features of tubular atrophy in man have been outlined in previous works (Chatelanat and Simon 1969; Flume et al. 1963; Maunsbach 1979; Ormos and Solbach 1963; Zollinger et al. 1973) but most investigations have been hampered by preparatory artifacts, which are present in renal biopsies necessarily fixed

by immersion. Hence, to circumvent this problem in the present investigation, we have developed a perfusion-fixation method applicable to nephrectomy specimens, a method which provides improved ultrastructural preservation of the human renal cortex (Maunsbach 1979; Møller et al. 1982).

Materials and methods

All kidneys examined in this study were derived from unilateral nephrectomies carried out for different therapeutic reasons.

Control kidneys. Kidney tissue from macroscopically and light microscopically normal parts of eight human kidneys served as control material. The control group included one kidney with a few cortical cysts, two kidneys with small, non-invasive pelvic papillomas (normal urograms apart from the tumour process) and five kidneys with small renal tumours which left the main parts of the kidneys macroscopically normal. In particular there was no tumorous involvement of the main renal vessels. The age of the patients varied from 46 to 86 years (mean age 61.9 years) and there was an equal distribution with respect to sex. All patients had a blood pressure within normal limits (<140/80 mm Hg), none had proteinuria and none was diabetic.

Hydronephrotic kidneys. Nine kidneys from nine patients with unilateral hydronephrosis of varying degrees were used for the study of proximal tubule atrophy. The remaining excretory function of the hydronephrotic kidneys, as measured by the clearence of I^{131}-Hippuran, ranged from 0–20% of total kidney function. The average width of the remaining parenchyma (cortex + medulla) was 13.8 mm (range: 2.0–25.0 mm) while the corresponding variables for the control group were 21.2 mm (range: 15.0–25.0 mm). Kidneys with pus in the renal pelvis or with abscess formation in the kidney tissue were not used. The age of the patients varied from 19 to 77 years (mean age 61.4 years), five patients were men and four women. All of the patients had a blood pressure within normal limits, none had proteinuria and none was diabetic.

Preparation for light and electron microscopy. All kidneys were perfusion-fixed within 15 min after interruption of the blood supply according to the procedure reported previously (Møller et al. 1982). The fixative consisted of 2% glutaraldehyde in 0.1 M cacodylate buffer to which was added 2% Dextran T 40 (Pharmacia, Uppsala) and had a total osmolality of approximately 400 mOsm/kg H_2O. Perfusion with the fixative was preceded by a short rinse with a Tyrode's solution containing 0.006% papaverine. Immediately after perfusion-fixation macroscopically well fixed tissue, which was hard and devoid of blood, was excised from the kidney and kept overnight at 4° C in the same fixative without dextran. In tumour kidneys the specimens were taken at least 20 mm away from the tumour process. Tissue blocks representing the entire cortical width were divided into two equal halves for light and electron microscopy, respectively. Paraffin-embedded sections were stained with haematoxylin and eosin. Specimens for electron microscopy were cut into 1 mm cubes, postfixed in 1% osmium tetroxide, stained *en bloc* with uranyl acetate and embedded in Epon. Semithin (1 μm) sections were stained with toluidine blue. Ultrathin sections were mounted on formvar-coated one-hole grids, stained with uranyl acetate and lead citrate and examined in a JEOL 100B electron microscope at 80 Kv using magnifications from 1000 × –30000 ×.

Histochemical preparation. Lysosomes were identified by incubation of glutaraldehyde-fixed cortical tissue for acid phosphatase in the Gomori medium as modified by Barka and Anderson (1962).

Selection of cortical areas for electron microscopy. Since, in perfusion-fixed tissue from human kidneys, occasional cortical areas appeared less well perfused, a primary selection of cortical

tissue for electron microscopy had to be done on the basis of the paraffin-embedded sections cut from tissue adjacent to that sampled for electron microscopy. Thus, a general criterion for acceptance of tissue for electron microscope analysis was a satisfactory quality of fixation, including largely blood-free vessels and predominantly open tubular lumina. An additional criterion in controls was the absence of inflammatory cell infiltrates and pathological changes in the vessels as well as the presence of only occasional sclerotic glomeruli. Tissue from hydronephrotic kidneys was accepted provided there were no polymorphonuclear leucocytes and only a moderate number of mononuclear inflammatory cells. The final selection of tissue for electron microscopy was made on semithin sections from cortical areas immediately adjacent to those accepted by the primary light microscopic screening. One area, approximately 200×300 μm, was chosen for ultrathin sectioning from each of four such semithin sections per kidney in such a way that each area contained at least two profiles of proximal convoluted tubules cut at right angle to their axis. Thus, in each kidney a total of at least 8 proximal tubule profiles were analysed. In case of severe tubular atrophy only such tubular profiles were analysed which from remnants of brush border could be safely identified as belonging to proximal tubules. No attempt was made to distinguish between the segments (S1 and S2) of the proximal convoluted tubules. However, the pars recta, which predominantly consists of the third segment (S3), was excluded as far as possible by avoiding medullary rays and by chosing proximal tubules situated close to a glomerulus. From each ultrathin section electron micrographs were obtained from at least two proximal tubule profiles and analysed systematically with respect to ultrastructure. Particular attention was paid to the relative amounts and relationships of normal or abnormal cell constituents. A total of about 2000 electron micrographs were analysed in this investigation.

Results

By light microscopy renal tubules in control tissue showed a normal appearence. They were uniformly distributed and separated by a narrow interstitial space. The light microscopic appearence of cortical tissue from hydronephrotic kidneys varied depending upon the degree of hydronephrosis. Thus, in slight hydronephrosis pathologically changed tubules were present only in minor cortical areas, the remainder of the tubules being light microscopically indistinguishable from normal ones. In severe hydronephrosis almost the entire population of tubules showed pathological changes such as reduced outer diameters and decreased epithelial height. The degree of tubular change varied from one cortical area to another. However, within limited regions such as those examined by electron microscopy the tubular changes as a rule showed no major differences. Dilatation of the proximal tubules was not a conspicuous feature in any of the hydronephrotic kidneys. In contrast, proximal tubules with collapsed lumens were frequently observed, particulary in cases of slight and moderate hydronephrosis.

The ultrastructure of proximal convoluted tubules in the control kidneys (Fig. 1) corresponded to that previously described in immersion-fixed biopsies (Ericsson et al. 1965 and 1967; Flume et al. 1963; Tisher et al. 1966) and was identical to that of perfusion-fixed human kidneys (Maunsbach 1979; Møller et al. 1982). Hydronephrotic kidney tissue representing cortical areas with light microscopic evidence of tubular and interstitial changes contained proximal tubules with varying degrees of ultrastructural simplification. The cells of such tubules were characterized by a reduced cell height, a loss of microvilli, a decreased complexity of basolateral membranes and a reduced number of cell organelles, in particular mitochondria (Figs. 2–4).

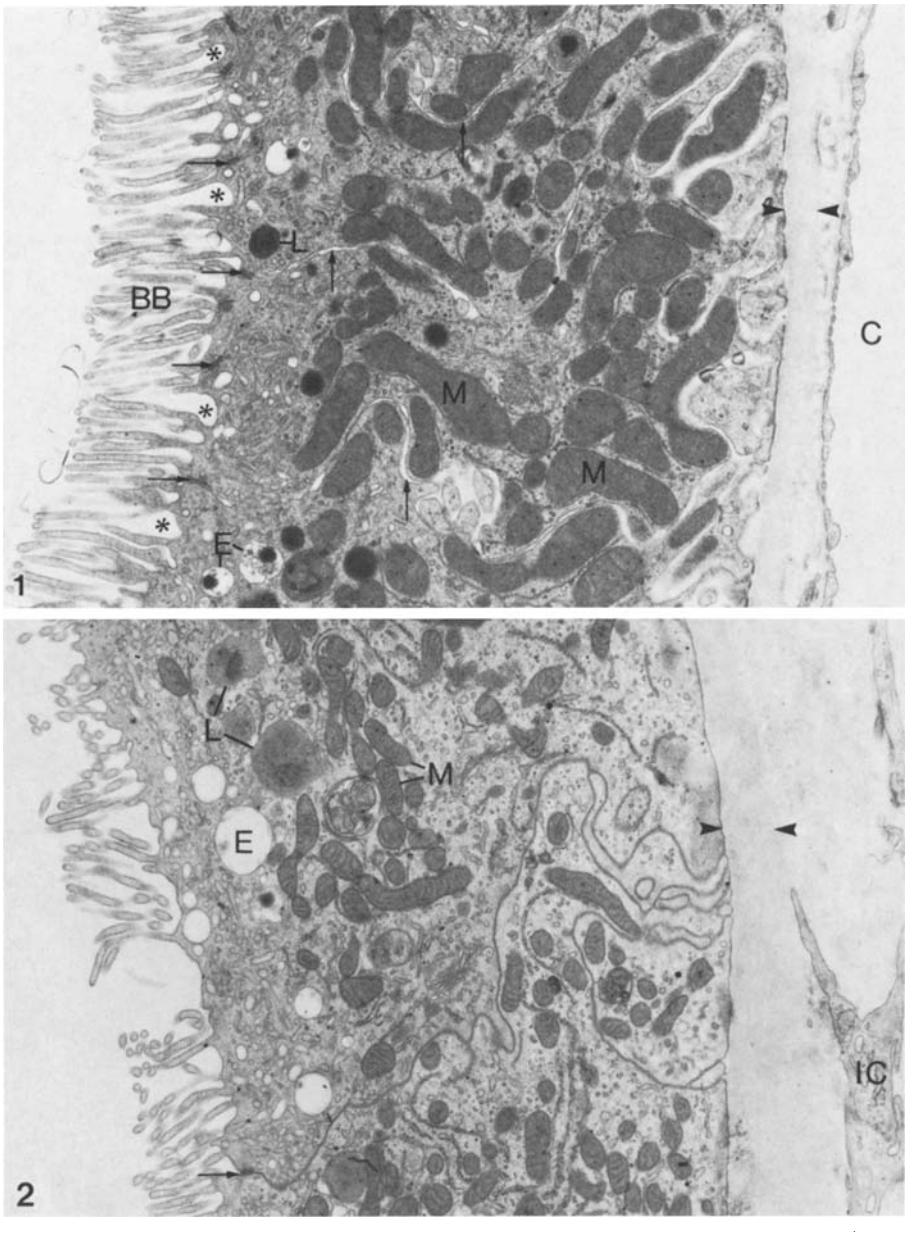

Figs. 1–4 show proximal tubules with increasing degrees of atrophy

Fig. 1. Cells of control proximal tubule showing regular brush border (*BB*), many apical endocytic invaginations (*asterisks*) and elongated mitochondria (*M*) oriented mainly perpendicular to the basement membrane, which is located between the arrowheads. Endocytic vacuoles (*E*) may be empty or show electron dense inclusions. There are several tight junctions (*horizontal arrows*) and complex interdigitations of basolateral membranes (*vertical arrows*). Note the close association between the tubule and the peritubular capillary (*C*). *L*, lysosome. ×9,000

Fig. 2. Tubule cells from slightly atrophic proximal tubule. The tubule cells are slightly reduced in height, the brush border is lacking focally and apical endocytic invaginations are less conspicuous than in controls. Some large endocytic vacuoles (*E*) are increased in size but generally lack electron dense inclusions. The mitochondria (*M*) appear reduced in number and size and many tend to be oriented parallel to the basement membrane (*between arrowheads*). There are only few tight junctions (*arrow*). *L*, lysosomes; *IC*, interstitial cell. ×9,000

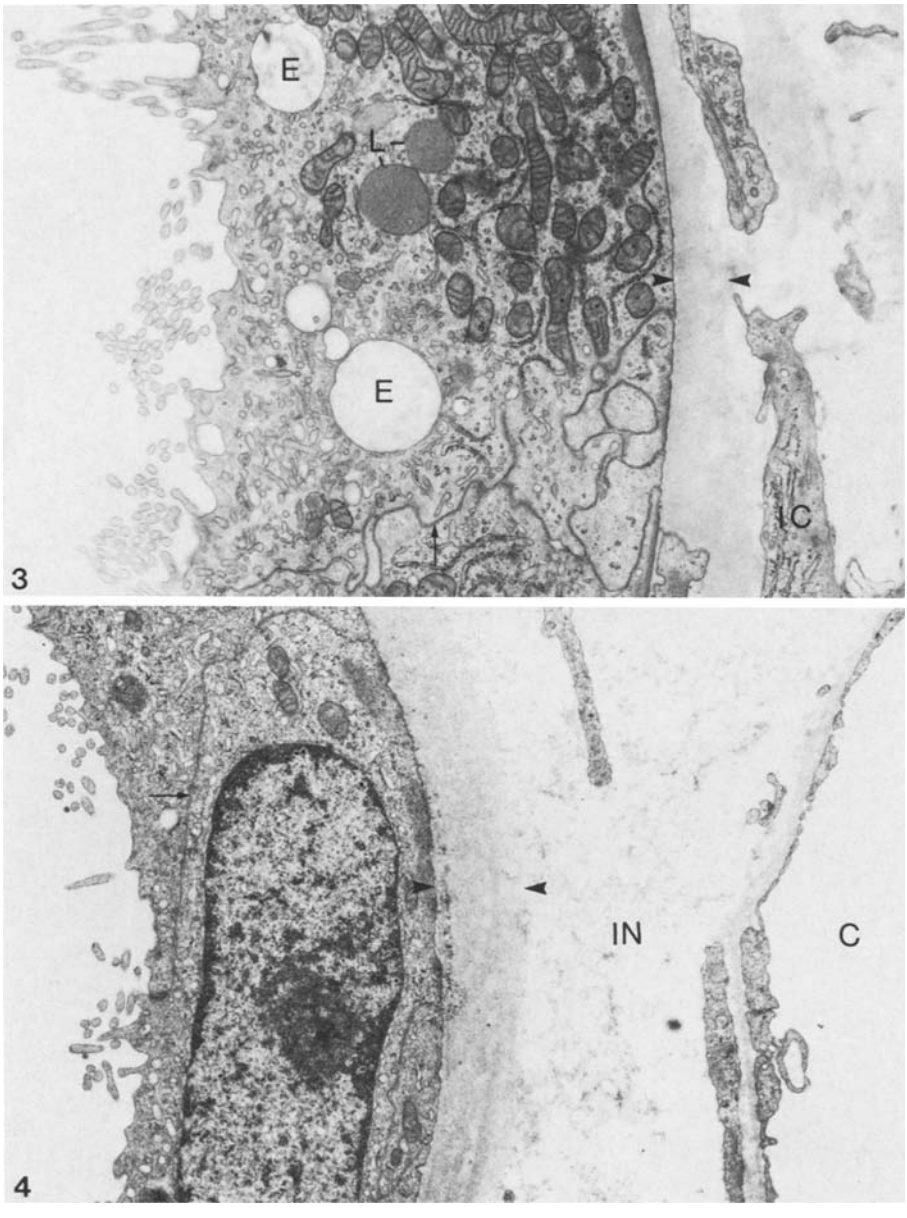

Fig. 3. Moderately atrophic tubule cells showing further decrease in cell height and loss of brush border. Large endocytic vacuoles (*E*) are prominent. Note the simplification of the interdigitation of basolateral membranes (*arrow*) and abnormal orientation of mitochondria. *L*, lysosomes; *IC*, interstitial cell. ×9,000

Fig. 4. Severely atrophic tubule cells with rudimentary brush border, almost no endocytic vacuoles and few mitochondria and other organelles. The lateral cell membranes (*arrow*) run in part parellel with the thickened basement membrane (*between arrowheads*). Note increased distance to peritubular capillary (*C*). *IN*, interstitium. ×9,000

At the light microscopic level it was impossible to establish useful criteria for allocation of individual proximal tubule profiles to particular subgroups representing different degrees of atrophy, and clear structural definitions of tubular atrophy have not been presented in the literature. In the following we therefore use the general terms "slight atrophy", "moderate atrophy" and "severe atrophy" based on an arbitrarily defined scale taking into account the sum of *ultrastructural* changes of several cell constituents. This was possible, since there was a large degree of parallelism between the severity of cellular changes at the different levels of atrophy, although, occasionally, deviations from this rule were noted. In the following we will describe separately the changes during atrophy in the various cell components and in the peritubular tissue.

Brush border. In control tubules the microvilli of the brush border were regularly arranged, approximately 2.5 μm in length, and exhibited thin internal filaments (Figs. 1, 5). With increasing tubular atrophy there was a gradual change of the brush border. In slight degrees of atrophy the changes were usually inconspicuous with only focal loss of microvilli (Fig. 2). With further atrophy still larger areas of the luminal surface appeared devoid of microvilli, and remaining microvilli were much reduced in length (Figs. 3–4). In spite of this modification of the microvilli they still contained thin internal filaments similar to those of normal microvilli (Figs. 6–7).

Basolateral membranes. The organization of the basolateral membrane, and thus cell shape, was considerably altered in atrophy. In general, the complex folds of the basolateral membranes, which are typical of tubule cells in the convoluted part of the mammalian proximal tubule (Figs. 1, 8, 11), became increasingly simplified with increasing degrees of atrophy. In moderate atrophy the small interdigitating cytoplasmic processes, which are particularly abundant immediately adjacent to the basement membrane in control tubules (Fig. 8), were few and the remaining processes broader than in controls (Fig. 9). Large parts of the basolateral membrane ran parallel with the basement membrane. Also the lateral borders between cells were simplified, as evidence of a lesser degree of lateral cellular interdigitation (compare Figs. 1 and 2). In severe atrophy the tubule cells showed low, cuboidal shapes with almost no basal interdigitating processes (Fig. 10) and reduced lateral interdigitation (Fig. 12). In some atrophic tubule cells the lateral cell borders showed a characteristic meandering pattern in sections cut at right angle to the basement membrane indicating that the lateral parts of the cytoplasm formed interdigitating folds which were oriented approximately parallel to the basement membrane (Fig. 13).

Cell junctions. The ultrastructure of tight junctions, intermediate junctions and desmosomes was similar in control and atrophic tubules.

Nuclei. The nuclei of control tubules appeared round or oval with an even nuclear envelope, a dispersed chromatin distribution and one or two small

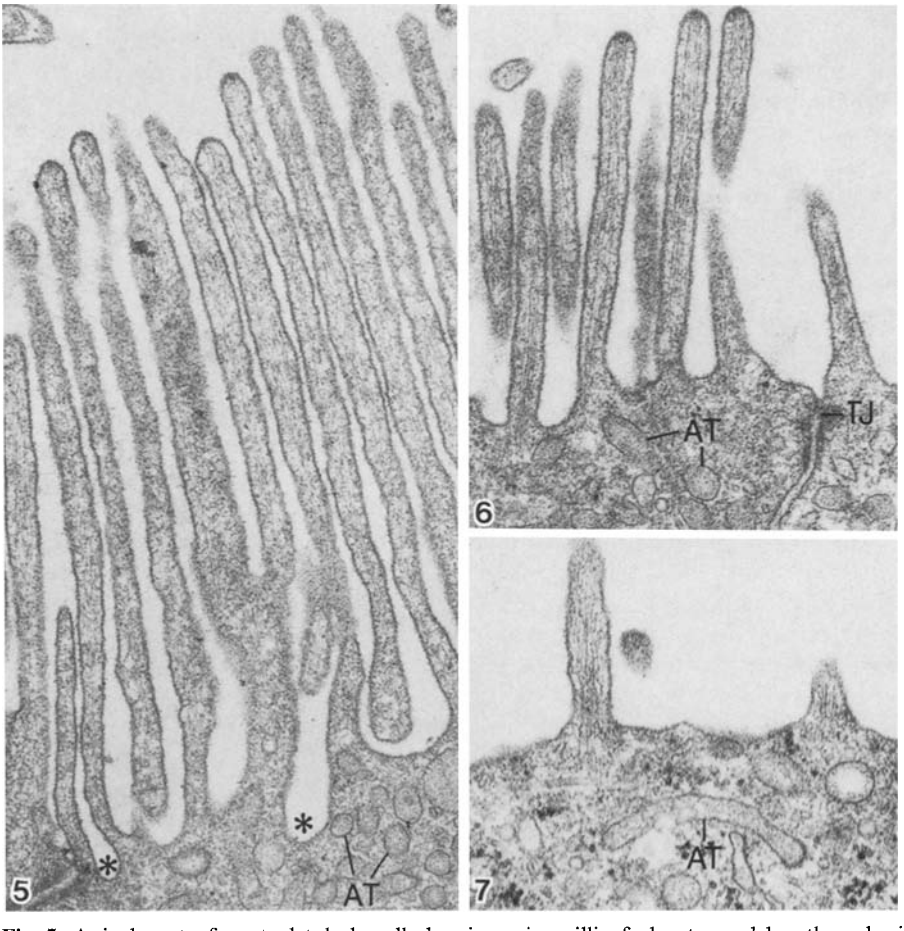

Fig. 5. Apical part of control tubule cell showing microvilli of about equal length and with delicate internal filaments. The apical cytoplasm contains endocytic invaginations (*asterisks*) and apical tubules (*AT*). × 36,000

Fig. 6. Apical part of moderately atrophic proximal tubule cell. Microvilli appear much reduced in length and of unequal size but show preservation of normal substructure, including internal filaments. *AT*, apical tubules; *TJ*, tight junction. × 36,000

Fig. 7. Brush border of severely atrophic proximal tubule cell with small, rudimentary and widely spaced microvilli. Note absence of endocytic invaginations. *AT*, apical tubule. × 36,000

nucleoli. In atrophic tubules the nuclei were flattened in parallel with the reduction in cell height. They had a more irregular outline and the chromatin often appeared irregularly distributed. Nucleoli were generally small, but some atrophic tubule cells showed nuclei with large nucleoli. There was no obvious difference between control and atrophic tubules as to the number of cell nuclei, which could be observed in individual tubule cross-sections. Mitotic figures were never observed.

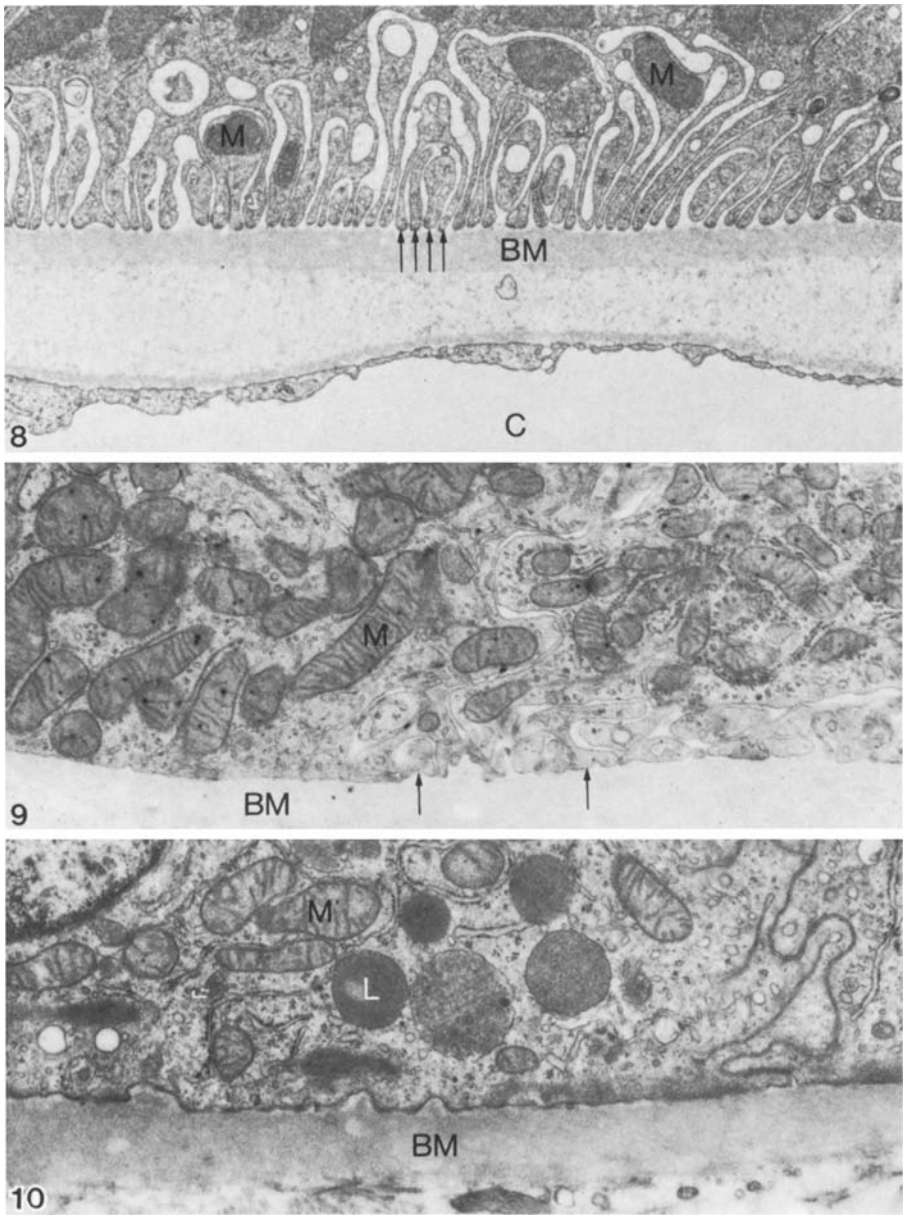

Fig. 8. Basal part of control proximal tubule cell showing numerous small interdigitating cytoplasmic processes (*arrows*) separated by narrow lateral intercellular spaces. Mitochondria (*M*) are closely associated with the basolateral membranes. *BM*, basement membrane; *C*, peritubular capillary. × 13,000

Fig. 9. Basal parts of moderately atrophic proximal tubule cells showing only few interdigitating processes (*arrows*). *M*, mitochondrion; *BM*, basement membrane. × 13,000

Fig. 10. Basal part of severely atrophic proximal tubule cell which is completely devoid of basal interdigitating processes. Mitochondria (*M*) are usually not associated with the cell membranes. *L*, lysosome; *BM*, basement membrane. × 13,000

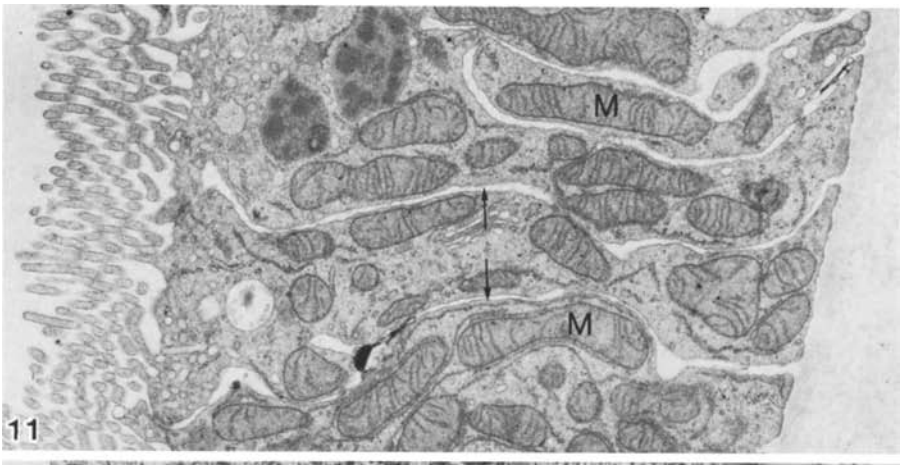
M
M
11

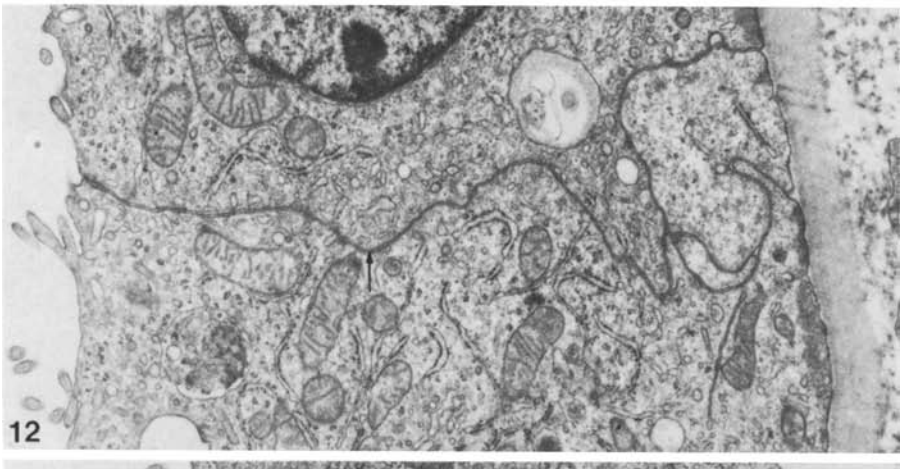
12

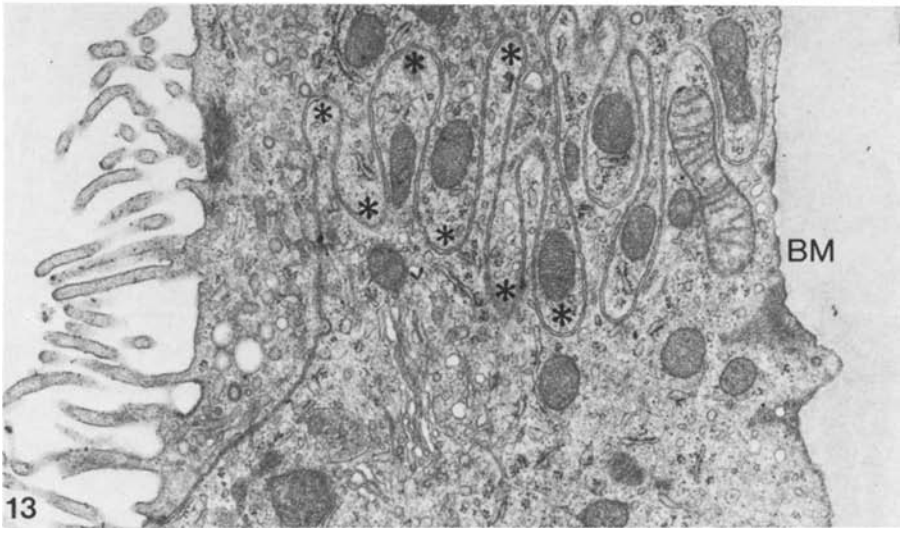
BM
13

Peroxisomes. Cytoplasmic bodies similar to those identified as peroxisomes in previous studies of human proximal tubule cells (Tisher et al. 1966) were observed in control tubules, often in association with cisternae of the endoplasmic reticulum. With increasing tubular atrophy peroxisomes gradually decreased in frequency, but remaining peroxisomes showed no ultrastructural differences from those of control tubules.

Mitochondria. In control tubules mitochondria were predominantly elongated, located in the basal half of the tubule cells and oriented approximately perpendicular to the basement membrane (Figs. 1, 11). They were closely associated with the basolateral membranes (Figs. 8, 11) and with the endoplasmic reticulum. With increasing tubular atrophy the mitochondria became reduced in number and size and gradually assumed a more round or oval shape (Figs. 2–4). A marked reduction in the number of mitochondrial profiles was obvious even in early stages of tubular atrophy (compare Figs. 1 and 2). Furthermore, the intimate association between mitochondria and basolateral cell membranes was gradually lost (Figs. 9, 10) and mitochondria tended to be oriented parallel to the basement membrane (Figs. 2–3). Changes of mitochondrial substructure were usually not observed (Fig. 14). However, in some atrophic tubules the remaining mitochondria appeared enlarged with an increased intercristal matrix (Fig. 15) and occasionally containing prominent bundles of filaments (Fig. 16).

Endoplasmic reticulum, Golgi complex. As compared with control tubules the cells of atrophic tubules usually showed a reduction in the amount of endoplasmic reticulum and in the number of Golgi complexes.

Apical invaginations and endocytic vacuoles. Control tubules showed numerous endocytic invaginations of the apical cell membrane, dense apical tubules as well as small vacuoles with a cytoplasmic coat. In addition the apical cytoplasm contained some large vacuoles, approximately 1 μm in diameter, and lacking a cytoplasmic coat (Fig. 17). Some of these vacuoles contained amorphous electron dense material and might be closely associated with lysosome-like bodies.

With the development of tubular atrophy and concurrently with the loss of microvilli there was a gradual reduction in the number of endocytic

Fig. 11. Part of control proximal tubule showing interdigitation between lateral processes of adjacent tubule cells. The cytoplasmic area, situated between the two intercellular spaces (*arrows*), represents a cytoplasmic process from one tubule cell which interdigitates with corresponding processes from another (or other) tubule cell(s). Note orientation of mitochondria (*M*) perpendicular to the basement membrane. × 10,000

Fig. 12. Adjacent cells of atrophic proximal tubule showing very little interdigitation of cytoplasmic processes (*arrow* on lateral cell membranes). × 11,600

Fig. 13. Meandering pattern of interdigitation in atrophic tubule. The interdigitating cytoplasmic folds (*asterisks*) are oriented parallel with the tubular basement membrane (*BM*). × 15,300

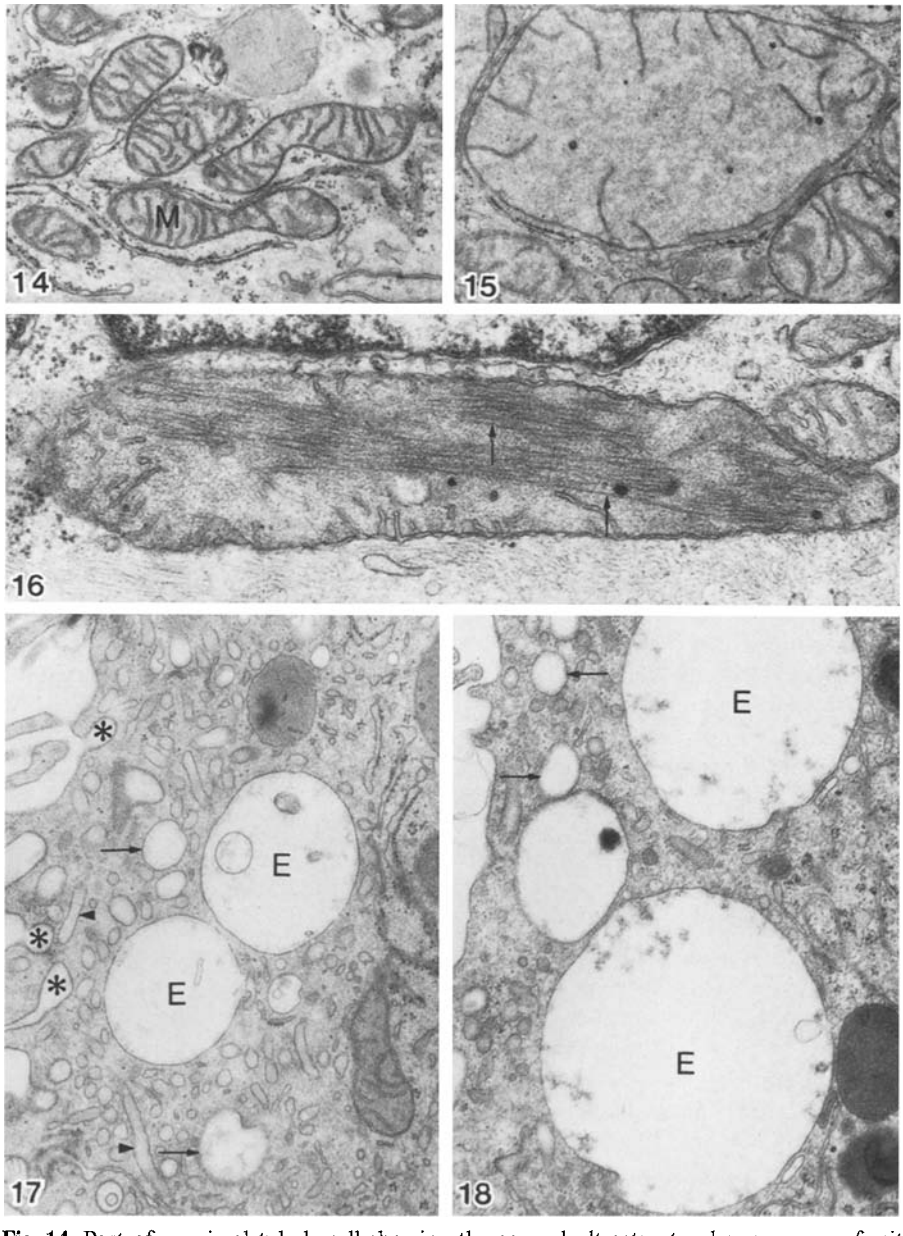

Fig. 14. Part of proximal tubule cell showing the general ultrastructural appearence of mitochondria (*M*) in atrophic tubules. × 20,000

Fig. 15. Giant mitochondrion with increased intercristal matrix. In cell of atrophic proximal tubule. For comparison with Fig. 14 note difference in magnifications. × 16,000

Fig. 16. Part of atrophic proximal tubule cell showing abnormal mitochondrion with bundles of filaments (*arrows*) in the matrix. × 32,000

Fig. 17. Endocytic-vacuolar system of control proximal tubule. Endocytic invaginations (*asterisks*) are present between the bases of the microvilli. The apical cytoplasm contains small endocytic vacuoles (*arrows*), large endocytic vacuoles (*E*) and small apical tubules (*arrowheads*). × 19,000

Fig. 18. Moderately atrophic proximal tubule cell showing large endocytic vacuoles (*E*) of increased size. Note a decreased number of apical endocytic invaginations as compared with controls. Small endocytic vacuoles (*arrows*) appear unchanged. × 19,000

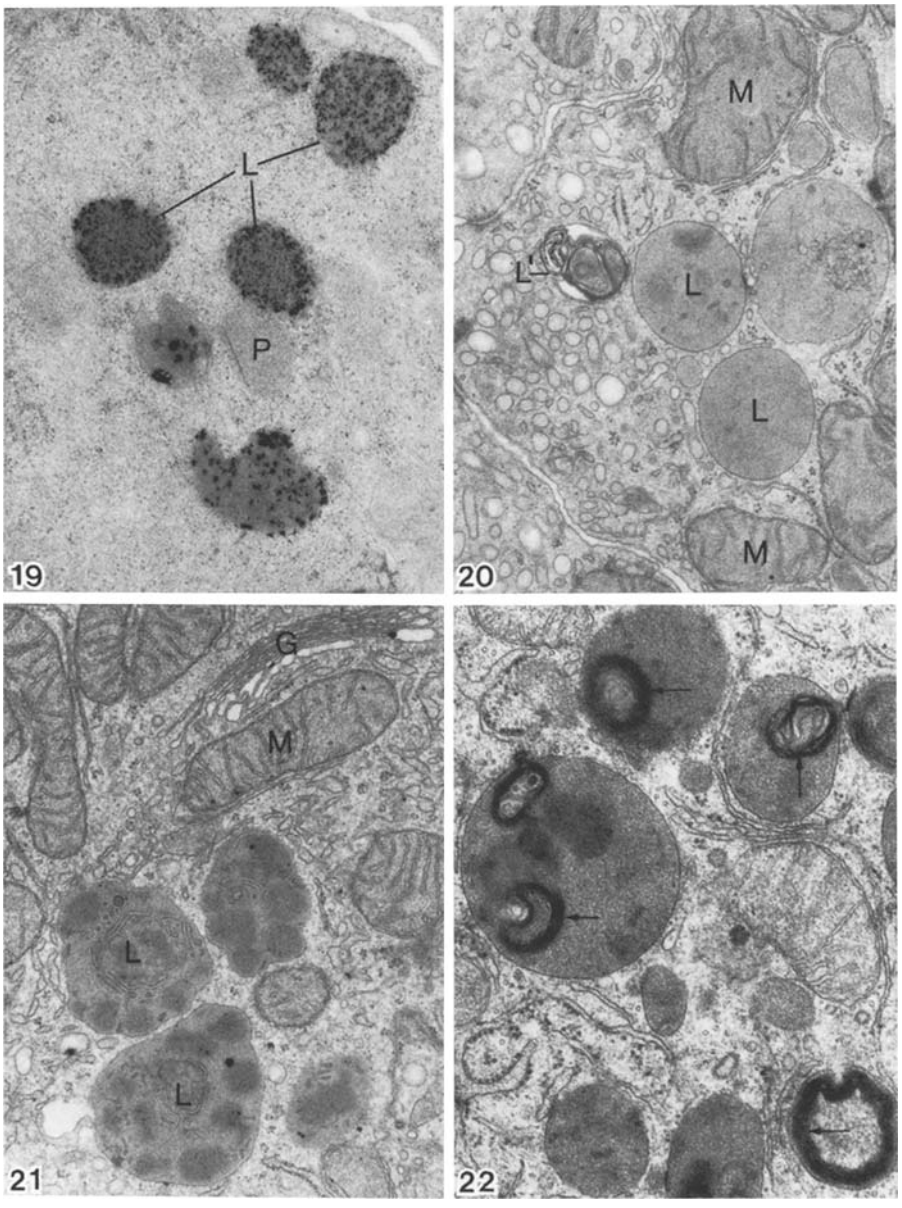

Fig. 19. Control proximal tubule cell in tissue incubated for acid phosphatase. Reaction product is present in several lysosomes (*L*), while a peroxisome (*P*) shows no reaction. ×16,000

Figs. 20–21. Control tubule cells illustrating the ultrastructure of various types of lysosomes (*L*). L′ probably represents an autophagolysosome. *M*, mitochondria; *G*, Golgi apparatus. ×19,000

Fig. 22. Part of moderately atrophic proximal tubule cell showing accumulation of single membrane limited bodies having inclusions in the form of whorls of membrane-like material (*arrows*). ×30,000

invaginations (Figs. 2, 3, 18). In most tubules the small coated vacuoles showed a corresponding reduction in number. However, in occasional tubule cells they appeared in increased numbers in spite of the presence of only few apical invaginations. In severely atrophic tubules small endocytic vacuoles were usually absent. A rather constant feature of slight and moderate tubular atrophy was the presence of increased numbers of large, uncoated vacuoles, which often appeared appreciably larger than those of control tubules (Fig. 18).

Lysosomes. Cells of control tubules contained cytoplasmic bodies, which in histochemical preparations showed acid phosphatase activity (Fig. 19), and which therefore were classified as lysosomes. The lysosomes varied in ultrastructure (Figs. 20–21) but appeared similar to those previously identified as lysosomes in the human proximal tubules (Tisher et al. 1966; Ericsson et al. 1967). With increasing tubular atrophy cytoplasmic bodies, which were ultrastructurally similar to those identified as lysosomes in control tubules, were gradually reduced in frequency. However, in slight and moderate degrees of atrophy single cells of some tubules showed an increased number of lysosome-like bodies, which were characterized by inclusions in the form of myelin-like whorls (Fig. 22). Lysosomes containing partly degraded, but still identifiable, organelles were encountered more frequently in atrophic tubules than in controls. The close spatial relationship between lysosomes and the Golgi apparatus was maintained through all stages of tubular atrophy, whereas contacts between lysosomes and large apical vacuoles were only rarely observed in atrophic tubules.

Filaments, basement membrane. Small bundles of filaments located at the base of the tubular cells and oriented parallel to the basement membrane were observed in some cells of control tubules. The filaments were 7–8 nm thick, thus resembling the actin filaments of smooth muscle in thickness (Kelly and Rice 1968). The bundles of filaments were between 0.1 and 0.3 μm in thickness. Neither the filaments nor the bundles of filaments showed any periodicity. Bundles of similar filaments were also present in atrophic tubules (Figs. 23–25). However, in particular in moderately atrophic tubules they occurred more frequently than in control tubules. Furthermore, they were larger in diameter, ranging in thickness from 0.2–0.5 μm. They were not confined to the base of the tubule cells and sometimes they traversed large parts of the tubule cell (Fig. 23). Some cells of atrophic tubules showed focal, peritubular outpouchings of cytoplasm and basement membrane. Bundles of filaments were often seen to extend from the margins of these cytoplasmic outpouchings, and in some sections the filaments seemed to separate basal portions of the cytoplasm from the rest of the tubule cell (Fig. 25). Furthermore, thick portions of the basement membrane of atrophic tubules sometimes showed granular inclusions.

Heterogeneity of atrophic tubule cells. In occasional cross-sections of atrophic proximal tubules there were single tubule cells which deviated in

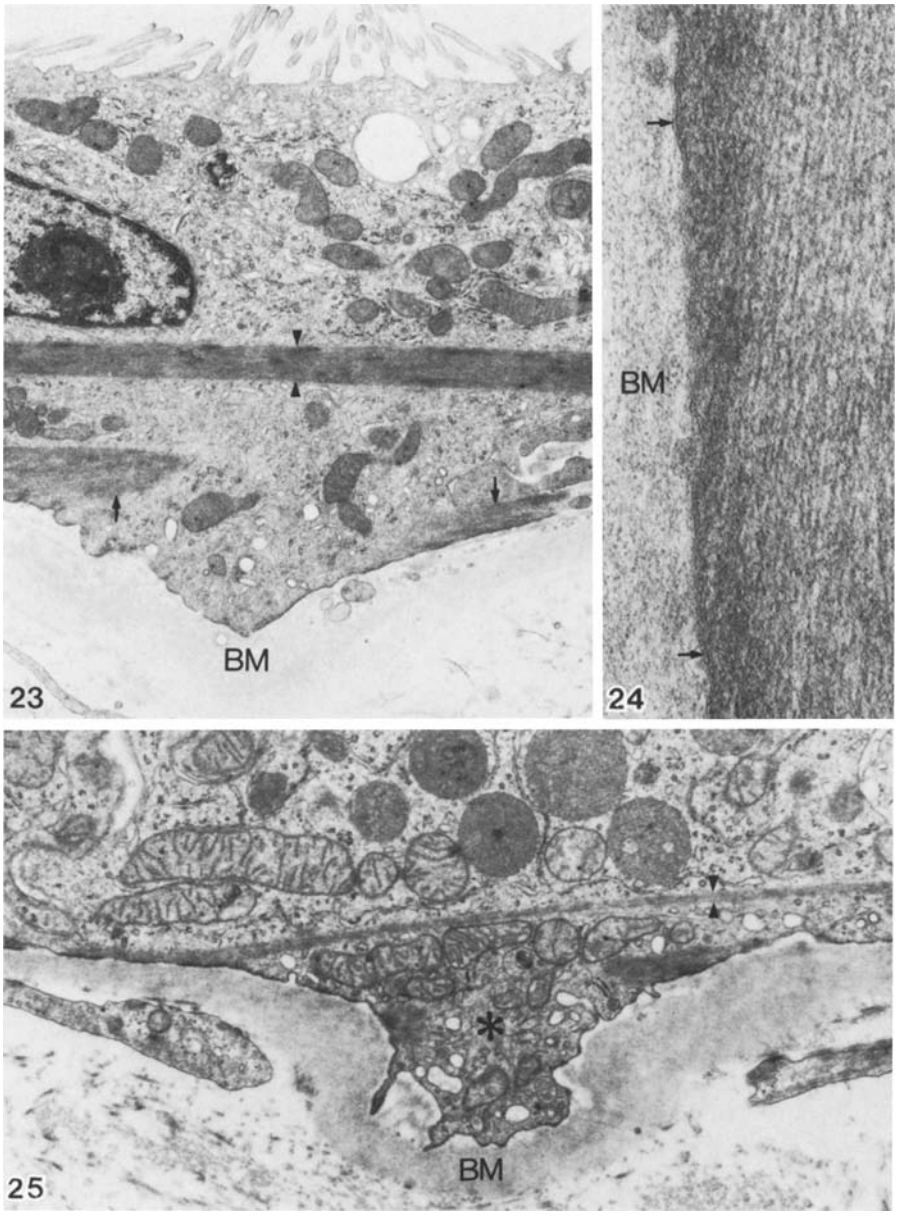

Fig. 23. Atrophic tubule cell showing large bundle of filaments (*between arrowheads*) traversing the cytoplasm. Additional bundles of filaments (*arrows*) are seen extending from the margins of an outpouching of the basal cell part and the basement membrane (*BM*). × 9,000

Fig. 24. Part of bundle of parallel, about 8 nm thick, filaments in atrophic proximal tubule cell. The filaments appear closely associated with the basal membrane of the tubule cell (arrows). *BM*, basement membrane. × 100,000

Fig. 25. Basal part of atrophic tubule cell showing outpouching of basement membrane (*BM*) and cytoplasm including various organelles (*asterisk*). A bundle of filaments (*between arrowheads*) separates the cytoplasmic outpouching from the rest of the cell. × 13,000

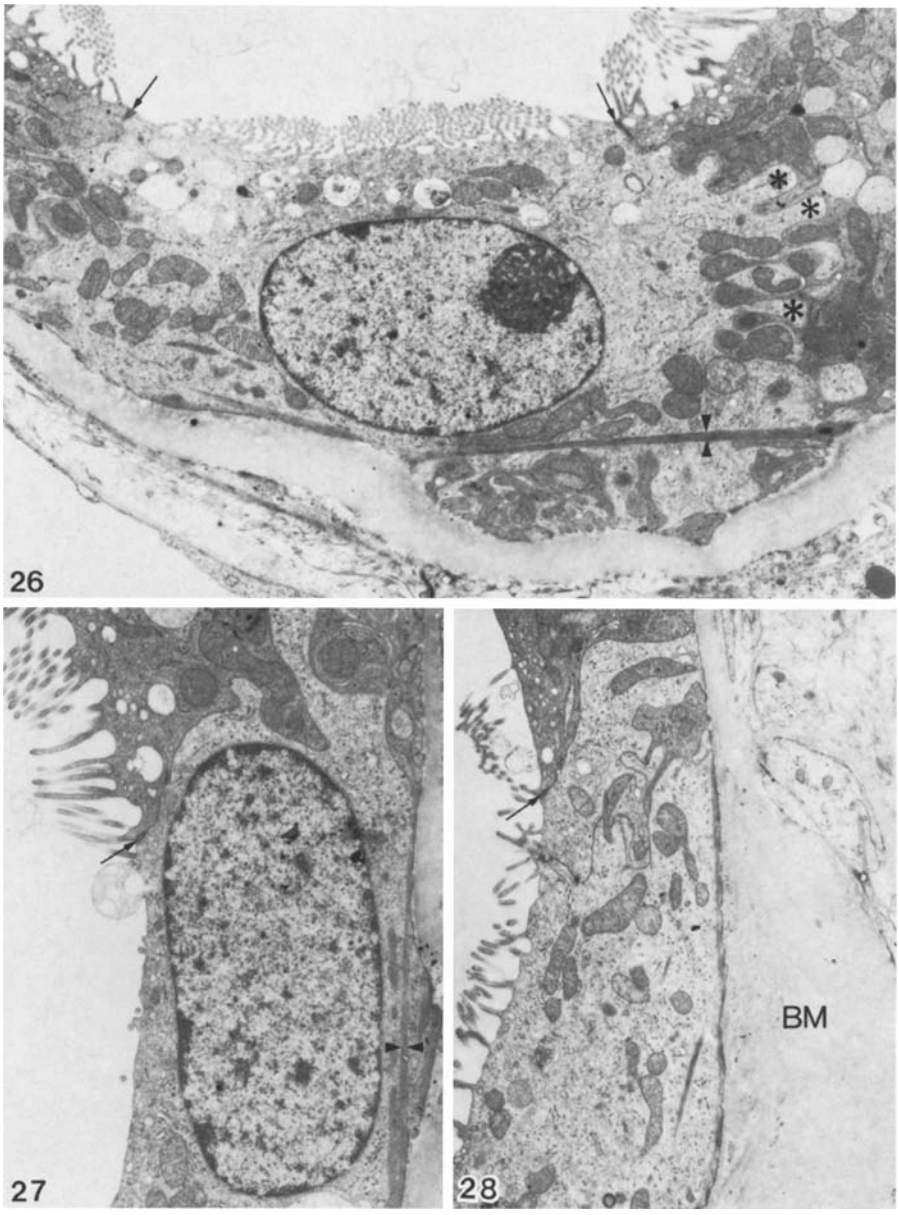

Figs. 26–28. Atrophic proximal tubule cells showing ultrastructural changes deviating from those of other cells of the same tubular cross-section. The borderlines at the lumen between these cells and adjacent tubule cells are indicated by arrows. Notice in particular the decreased cytoplasmic density of these cells, the very short (Fig. 26) or totally lacking (Fig. 27) microvilli and increased thickness of the basement membrane (*BM* in Fig. 28). Some of the cells have bundles of filaments (Figs. 26 and 27 between *arrowheads*) and occasional cells exhibit a meandering pattern of interdigitations between lateral cell processes (*asterisks* in Fig. 26). Fig. 26 × 5,200, Fig. 27 × 6,800 and Fig. 28 × 5,700

ultrastructure from the other tubular cells of the same cross-section. Thus, irrespective of the degree of tubular atrophy, these cells were characterized by a less dense cytoplasm than that of adjacent tubule cells and the microvilli were either totally lacking or considerably reduced in frequency and size (Figs. 26–28). Furthermore, the cells were devoid of basal interdigitations, but lateral cytoplasmic processes sometimes showed extensive interdigitations with neighbouring tubule cells in a plane parallel to the basement membrane (Fig. 26). Mitochondria, vacuoles and lysosomes were scarce, whereas free ribosomes occurred in increased numbers and often formed small rosettes. Bundles of filaments, ultrastructurally similar to those described above, were frequent in these cells (Figs. 26–27), which were further characterized by an appreciable thickening of the basement membrane (Fig. 28). The nuclei were often large with prominent nucleoli.

Cortical interstitium. The ultrastructural appearence of the cortical interstitium in controls corresponded basically with that described for the rat kidney (Pedersen et al. 1980). Thus, the interstitium could roughly be divided into two compartments: a wide interstitium located between tubules and containing interstitial cells mainly of "fibroblastic" type (Bohman 1983) and a narrow interstitium located between tubules and capillaries and devoid of cells. The topographical relationships between a given tubular cross-section and adjacent capillaries varied, but as a rule each tubule showed a close spatial association with at least one peritubular capillary with almost no intervening interstitial tissue (Fig. 29).

In the cortices of hydronephrotic kidneys the interstitium showed a variable degree of expansion, which was attributable mainly to an increased amount of amorphous ground substance. In slight degrees of interstitial expansion increase of interstitial tissue was usually most prominent in the wide interstitium. However, in moderate and severe degrees of interstitial expansion the narrow interstitium between tubules and capillaries was also involved. As a consequence the topographical relationships between tubules and capillaries were changed and tubulo-capillary distances increased (Fig. 30). Concurrently with the expansion of cortical interstitium fibroblastic cells appeared in increased numbers. These cells often encircled the tubules in part or the peritubular capillaries by means of long cytoplasmic projections (Fig. 30). Bundles of microfilaments, ultrastructurally indistinguishable from the 7–8 nm filaments described in the tubule cells, were frequently observed in such cytoplasmic projections and often in close apposition to the tubular basement membrane (Fig. 31).

Peritubular capillaries. The capillary endothelium of controls usually appeared as a thin cytoplasmic layer with numerous fenestrations (Figs. 29, 32). In slight degrees of tubular atrophy and interstitial tissue increase there were no obvious changes of the capillary endothelium. However, in more advanced stages of tubulo-interstitial disease the capillary endothelium was often thickened (Fig. 30) and showed a reduced number of fenestrations

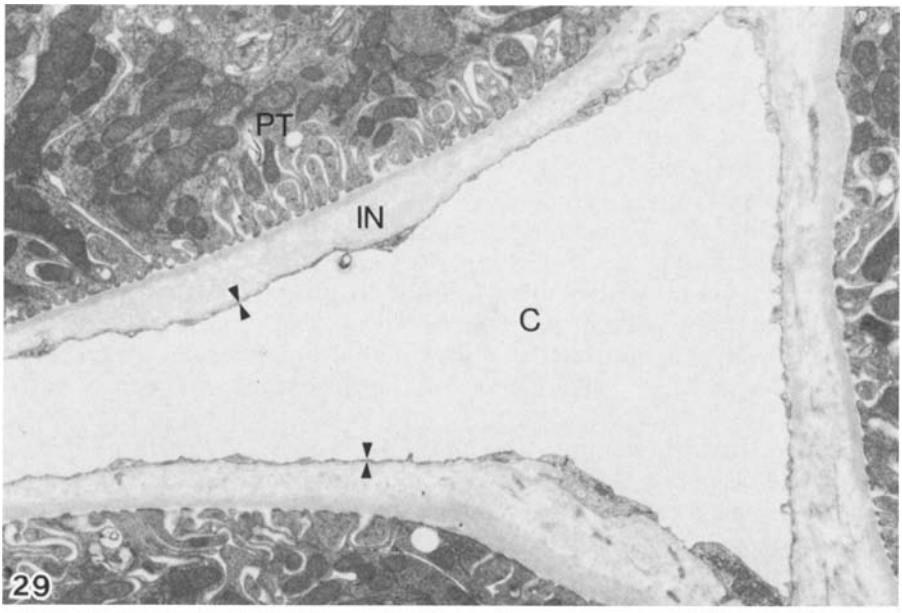

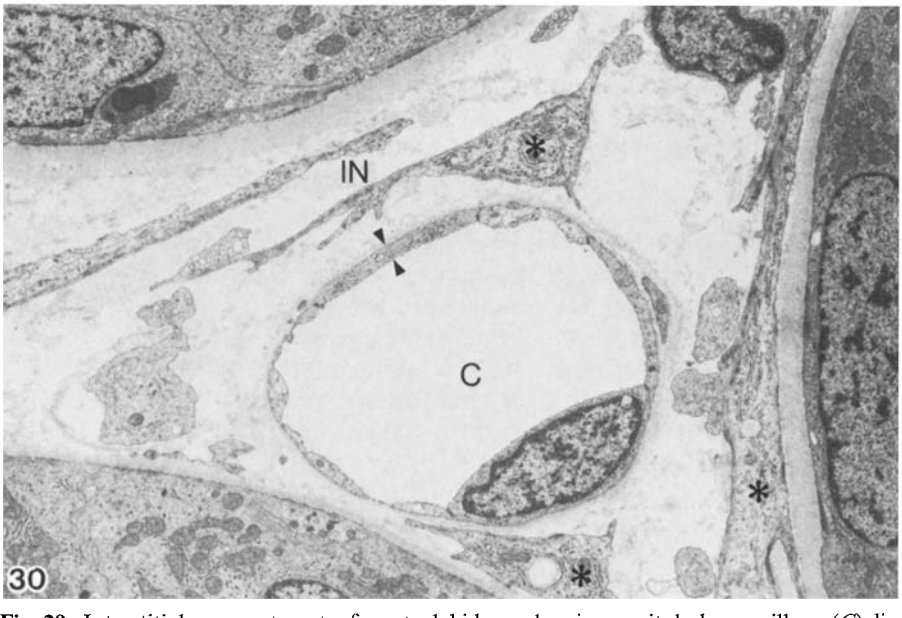

Fig. 29. Interstitial compartment of control kidney showing peritubular capillary (*C*) lined by a thin endothelial layer (*between arrowheads*). Note close spatial relationship between capillary and adjacent proximal tubules (*PT*). *IN*, interstitial connective tissue. × 5,300

Fig. 30. Interstitial compartment of atrophic kidney. Increased amounts of interstitial connective tissue (*IN*) in addition to fibroblasts (*asterisks*) with long cytoplasmic projections separate peritubular capillary (*C*) from surrounding tubules. Note increased thickness of peritubular capillary endothelium (*between arrowheads*). × 5,300

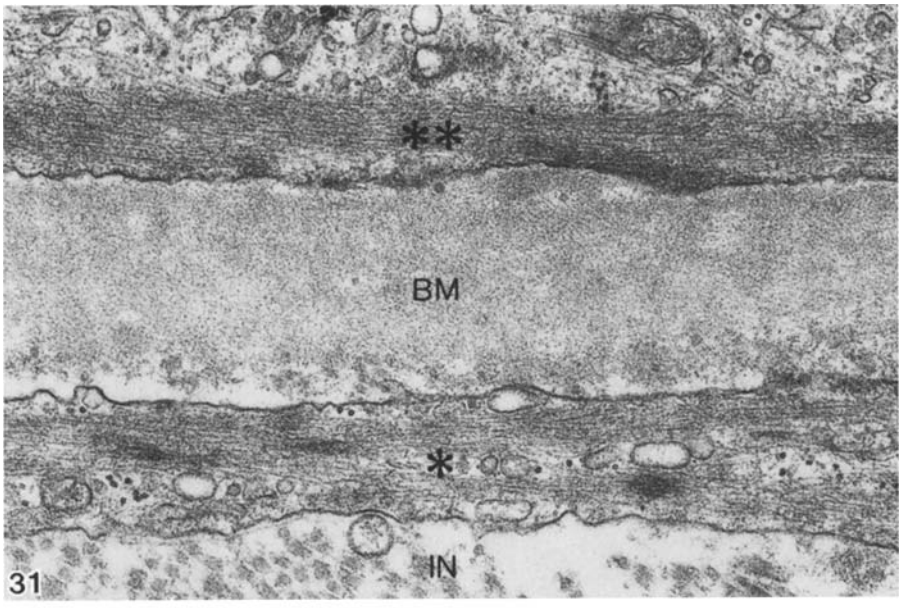

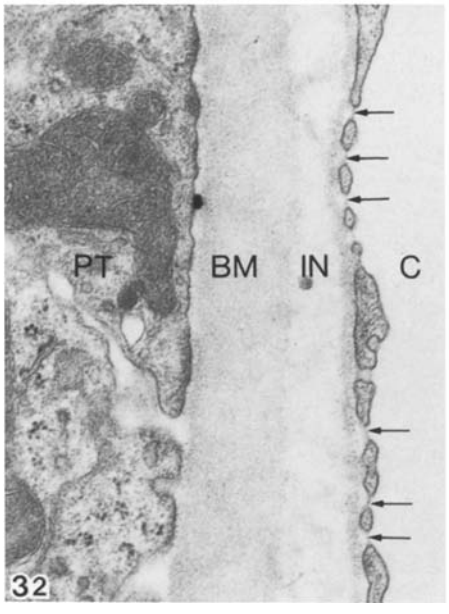

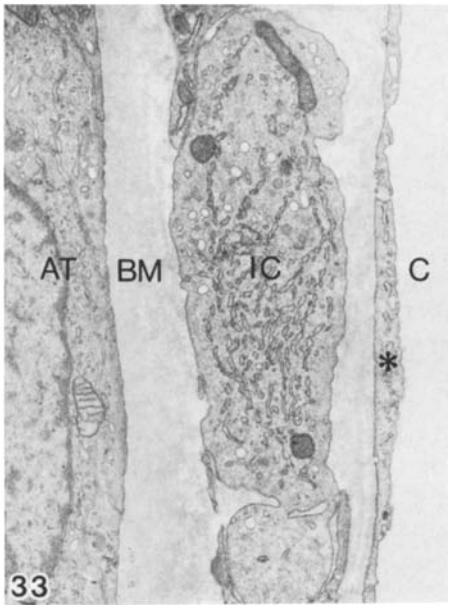

Fig. 31. Cytoplasmic projection from fibroblast (*single asterisk*) closely apposed to the basement membrane (*BM*) of atrophic proximal tubule. The projection show filaments, which are ultrastructurally indistinguishable from those located at the base of the tubule cell (*double asterisk*). *IN*, interstitium. × 36,000

Fig. 32. Peritubular capillary (*C*) of control kidney showing many endothelial fenestrations (*arrows*). The capillary wall has a close spatial relationship with the proximal tubule (*PT*) with almost no intervening interstitial tissue. *BM*, tubular basement membrane. × 30,000

Fig. 33. Peritubular capillary (*C*) of atrophic kidney cortex with thickened endothelium (*asterisk*) devoid of fenestrations. The capillary is separated from the atrophic tubule (*AT*) by interposition of an interstitial cell (*IC*), probably a fibroblast. For comparison with Fig. 32 note difference in magnifications. *BM*, tubular basement membrane. × 9,000

as compared with controls. This was particular the case, when the peritubular capillaries were separated from the tubules by accumulations of collagen fibers or by interposition of interstitial cells (Fig. 33).

Discussion

The present study demonstrates that proximal tubular atrophy in human hydronephrosis results in a series of ultrastructural changes involving almost all structural components of the tubular cells. It emphasizes that tubular atrophy is associated not only with a reduced number of cell organelles but also with a derangement of the complex architecture characterizing normal proximal tubular cells. However, since there is little direct information concerning the structure-function relationships in the human proximal tubule the functional implications of the observed structural changes must be derived from comparisons with analogous changes in experimental animals. This seems justified since the ultrastructure of the proximal tubule in man (Tisher et al. 1966; Maunsbach 1979) is basically similar to that of the rat (Maunsbach 1973) and the rabbit (Kaissling and Kriz 1979). In the following we will discuss the different ultrastructural changes of the human proximal tubule in atrophy and their possible functional implications.

Brush border. Reduction in the size and number of microvilli has been reported in human proximal tubular atrophy irrespective of the underlying disease (Farquhar et al. 1957; Flume et al. 1963; Gise et al. 1981; Maunsbach 1979). However, the present findings indicate that changes of the brush border are generally inconspicuous in early tubular atrophy, which is in agreement with observations in experimental hydronephrosis (Nagle et al. 1973a; Shimamura et al. 1966).

The mechanisms underlying the brush border loss in tubular atrophy are not clear. In the acutely ischaemic rat kidney the predominant changes in the brush border appear to be a distortion and swelling of microvilli (Glaumann et al. 1975; Venkatachalam et al. 1978), whereas, following reflow, there may be a marked loss of microvilli (Reimer et al. 1972). A similar massive reduction of the brush border has been described for proximal tubules in cases of acute renal failure in man (Olsen and Olsen 1983). Experimental evidence suggests that this acute brush border loss takes place both by an interiorization of microvilli in the tubule cells and also by a fragmentation and shedding of microvilli into the tubule lumen (Venkatachalam et al. 1978). Since, in the present study, atrophic tubules generally appeared devoid of luminal cell debris and images suggesting interiorization were never observed, similar mechanisms seem unlikely. However, it cannot be excluded that loss of brush border in tubular atrophy may proceed in part by a shedding of apical cell parts at a slower rate than in the acutely ischaemic kidney.

It is well known that the plasma membrane of the brush border contains a number of important transporting enzymes (Berger and Sacktor 1970).

Still, little is known of the physiological significance of the brush border, and the consequence for tubular function of various degrees of brush border loss cannot be predicted. However, there is some experimental evidence that an intact brush border is required for normal sodium and water reabsorption by the proximal tubules (Venkatachalam et al. 1978).

Basolateral membranes. It is generally accepted that active sodium transport across the peritubular cell membrane in the proximal tubule is the primary driving force for fluid reabsorption (for a review see Giebisch 1978). The sodium transport is mediated mainly by membrane-associated Na, K-ATPase (Katz 1982). It is therefore widely assumed that the capacity of the proximal tubule cells for ion and fluid transfer is correlated to the available area of basolateral membranes, a suggestion which is also directly supported by results of structure-function analyses in developing rat kidneys (Larsson and Horster 1976).

In atrophic human tubules the transport characteristics of the tubule cells have never been determined. However, on account of the observed pronounced decrease in basolateral interdigitations, and thus basolateral cell membrane area, with increasing proximal tubule atrophy it is conceivable that peritubular active sodium transport is reduced and fluid reabsorption consequently decreased.

Mitochondria. The qualitative changes in the mitochondria in tubular atrophy is a matter of controversy. Thus, according to some reports (Flume et al. 1963; Ormos and Solbach 1963) the mitochondria are swollen and show a reduced number of cristae and flocculent densities in the intercristal matrix. Similar mitochondrial changes have been demonstrated in tubule cells during autolysis (Latta et al. 1965) and in cells subjected to complete ischaemia (Mergner et al. 1976). However, it is also recognized that such mitochondrial changes may represent artifacts of fixation, in particular a result of delayed fixation of cells located at a distance from the surface of the fixed tissue block (Maunsbach et al. 1962). The present observations, which are based on perfusion-fixed tissue, demonstrate that the mitochondria of atrophic tubules, apart from modifications with regard to size and shape, appear structurally similar to those of controls. Therefore, swelling of mitochondria in atrophic tubules most likely represents an artifact of fixation rather than a true pathological lesion. Giant mitochondria, sometimes with filaments in the matrix, represent an exception. Such abnormal mitochondria have been observed previously (Suzuki et al. 1975; Thoenes 1966) but have not been associated with any specific type of tubular dysfunction.

Comparative structure-function studies on the developing proximal tubule (Larsson and Horster 1976) have provided evidence that tubular cell differentiation and maturation towards normal functional capacity is correlated not only with an increasing amount of mitochondria but also with a closer spatial relationship between mitochondria and basolateral cell membranes. The mitochondrial changes described here for atrophying tubules

appear to represent a reversal of the process observed in the developing proximal tubule. Thus, a reduction in the number of mitochondria and a disruption of the intimate association between mitochondria and basolateral membranes appears to be one of the very first and most obvious changes of the proximal tubule cells during the development of atrophy. Hence, it seems reasonable to assume that energy-requiring tubular functions, in particular salt and water reabsorption but also transport of glucose and amino acids, may be reduced even in relatively early stages of atrophy. However, it should be pointed out that the present observations allow no conclusions as to whether the tubular changes reflect an adaptive response to a reduced functional load or a sequel to other pathophysiologic stimuli.

Endocytic vacuoles and lysosomes. The present observation that proximal tubule atrophy in its more advanced form is associated with an overall reduction of endocytic vacuoles and lysosomes is in agreement with previous observations (Flume et al. 1963; Maunsbach 1979). In slight and moderate degrees of atrophy, on the other hand, the changes of the endocytic and lysosomal system showed a considerably more variable pattern. However, a general feature of early tubular atrophy appeared to be an increase in the number and size of large vacuoles. A similar reaction has been described for proximal tubules in experimental hydronephrosis (David 1963; Nagle et al. 1973a; Shimamura et al. 1966), in various types of human progressive renal disease (Flume et al. 1963) and in rats of advanced age (Christensen and Madsen 1978). The pathophysiologic basis for this cellular reaction is unknown, but increased vacuolization of proximal tubule cells has been produced experimentally in kidneys subjected to maleate (Christensen and Maunsbach 1980) or to ischaemia (Venkatachalam 1978), conditions which interfere with the enzymatic energy production required for normal protein absorption and transport in the tubule cell. The possibility that the increased formation of vacuoles, at least in part, reflects excess absorption of protein should also be considered. However, the general reduction of apical endocytic invaginations and small vacuoles, which according to tracer studies represent structural precursors of large vacuoles (Maunsbach 1966a), seems to speak against such a mechanism.

Lysosome-like cytoplasmic bodies containing lamellar material as observed in some cells of atrophic tubules of the present study have also been described in various types of acute toxic kidney injury e.g. following the administration of gentamicin (Wellwood et al. 1975). The pathogenetic basis for this reaction and its functional significance, in particular as concerns protein metabolism, are unknown. However, the results of histochemical studies of normal rat proximal tubules have indicated that cytoplasmic bodies with inclusions of lamellar material (cytoplasmic bodies type II with layered material) have less acid phosphatase activity than other subtypes of lysosomes (Maunsbach 1966b). Furthermore, in a recent study of experimental lipidosis cytoplasmic bodies containing lamellar material participated less in protein degradation than did normal appearing lysosomes (Christensen et al. 1983).

Filaments, basement membrane. Small bundles of filaments, ultrastructurally similar to those observed in the present control tubules, have been described as normal constituents of both human (Tisher et al. 1966) and animal (Pease 1968; Tisher et al. 1969) proximal tubule cells. In rat proximal tubule cells they have been identified as actin filaments (Rostgaard et al. 1972). Accumulations of such filaments at the base of the tubule cells have been observed in toxic lesions (David and Uerlings 1964; Myler et al. 1964), in acute renal failure (Jones 1982) and in regenerating epithelium (Ormos et al. 1973), but the precise pathophysiological stimulus for this reaction is unknown. Focal, hernia-like outpouchings of basement membrane with trapping of basal cell parts comparable to those observed here in human atrophic tubules have been noted also in various experimental conditions leading to tubular atrophy (Anderson 1963; Romen and Mäder-Kruse 1978). This change has been suggested to represent a sequel to shrinkage of the tubules and a contributary factor in the development of basement membrane thickening. The present findings are consistent with this possibility. However, the occurrence in atrophic tubules of large bands of filaments in close structural relation to hernia-like extensions of the basement membrane also raises the possibility that contraction of tubule cells plays an active role in adjusting the diameter of the tubule lumen to the intratubular pressure, which may be reduced in chronic experimental hydronephrosis (Wilson 1980). Myosin filaments were not demonstrated, but this might be due to the need for special preparatory methods for the visualization of this type of filaments (Rostgaard et al. 1972).

Interstitium, capillaries. The qualitative changes described here for the cortical interstitium are in accord with the findings in experimental hydronephrosis (Nagle et al. 1973a). Proliferation of fibroblasts appears to be an early event following ureteral obstruction (Nagle et al. 1976). The tendency of these cells to encircle the tubules and capillaries in addition to the supposed contractile properties of their filaments (Nagle et al. 1973b) indicate that interstitial cells may have significant influence on the progressive course of tubular atrophy in chronic renal disease. This might be achieved by changing the local microcirculation (Nagle et al. 1973b) or by way of pure mechanical obstruction to the exchange of solutes and gasses between tubules and capillaries due to interposition of interstitial cells. This latter possibility finds support by the present observation that the endothelium of peritubular capillaries is often thickened and devoid of fenestrae in places where interstitial cells are interposed between capillary and tubule. Furthermore, recent experimental observations indicate, that proliferation of cortical interstitial cells is associated with increased production of prostaglandin (Bernard et al. 1983), which has been suggested a possible mediator of changes of cortical blood-flow in the chronically obstructed kidney (Wilson 1980).

Tubular atrophy – regressive changes or imperfect regeneration?

The ultrastructural changes, which have been described here for atrophic proximal tubules, may be interpreted in two principally different ways. On

one hand, they may represent sequels to a gradual, degenerative process eventually leading to the formation of tubule cells of simplified and dedifferentiated structure. Alternatively, atrophy may be a sequel to a regenerative process, where the differentiation of tubule cells remains incomplete.

Degenerative, ultrastructural changes of known aetiology have been studied almost exclusively in short term experiments. Thus, proximal tubules of acutely ischaemic rat kidneys show distortion and swelling of microvilli in addition to condensation and later swelling of mitochondria eventually with disruption of mitochondrial membranes (Glaumann et al. 1975; Mergner et al. 1976). Following re-flow, there may be a loss of microvilli and an increased formation of vacuoles and secondary lysosomes (Dobyan et al. 1977; Glaumann et al. 1977) as is also observed in human proximal tubules during acute renal failure (Olsen and Olsen 1983). In cases of nephrotoxic injury due to for example mercuric chloride (Cuppage and Tate 1967), gentamicin (Houghton et al. 1976; Wellwood et al. 1975) or maleic acid (Verani et al. 1982) proximal tubule cells may show somewhat similar changes of cell organelles. However, in nephrotoxic injury changes of the lysosomal system are often predominating as demonstrated in particular for the gentamicin model (Dobyan et al. 1982).

The ultrastructural changes observed in atrophic tubules in this investigation do not resemble those characterizing tubules in acute ischaemia. In particular distortion of microvilli was not a distinctive feature, though loss and shortening of microvilli was observed. Furthermore, the mitochondrial changes of acutely degenerating tubule cells are usually quite different from the changes observed here in atrophic tubules, which mainly consist of a reduction of the number and size of the mitochondria. The only changes of proximal tubules that resemble those observed in acutely degenerating tubules were related to the vacuolar apparatus and the lysosomal system. Thus, increased formation of vacuoles and accumulation of osmiophilic, lamellar material in vacuoles and lysosomes appear to be common features. However, while lysosomal changes are usually outstanding features of acutely degenerating tubule cells, they are inconsistently present in atrophic tubules and often confined to single tubule cells.

The sequence of ultrastructural changes, which have been described for various stages of tubule cell *regeneration* (Cuppage and Tate 1967; Kempczinski and Caulfield 1968; Houghton et al. 1976; Ormos et al. 1973) as well as for the differentiation of the developing proximal tubule (Clark 1957; Larsson 1975) appears to be in many respects a reversal of the changes characterizing increasing degrees of proximal tubule atrophy. Thus, in regenerating tubule cells there is a gradual increase in organelles and formation of basolateral interdigitations. Interference with this process, therefore, may lead to various degrees of incomplete regeneration. Whether or not regeneration of cells takes place in atrophying tubules is difficult to assess on a morphological basis. In the present series necroses of tubule cells were only rarely encountered and mitotic figures not at all, which seems to indicate that cell death and renewal is at a low rate in chronic renal disease. However, it has been shown that there is an increased incorporation of tritiated thymi-

dine in the tubular cells during early stages of hydronephrosis in rats (Benitez and Shaka 1964). The present observations show that in human atrophic tubules there are cells, which have an ultrastructural appearence corresponding to that described for early regenerating tubule cells, including total lack of or only scarcely developed microvilli, an increased number of ribosomes and in some cases bundles of filaments. Therefore, it appears likely that attempts at regeneration may take place in atrophic tubules and that some cells of simplified structure represent regenerating cells in various stages of imperfect differentiation.

We conclude that both incomplete regeneration and degenerative changes may contribute to the atrophic state of tubules in chronic human hydronephrosis, although the extent to which each of these two processes are involved in tubular atrophy remains to be established.

There is circumstantial evidence that in physiological conditions the glomerular filtration rate (GFR) is adjusted by way of a tubulo-glomerular feed-back mechanism, which is mediated by the macula densa cells of the juxtaglomerular apparatus and effected by the vasoconstrictive properties of renin-angiotensin on the afferent glomerular arteriole (Wright and Briggs 1979). The factor responsible for the feed-back response was originally thought to be the sodium load on the macula densa cells (Thurau and Schnermann 1965), but later experimental observations have pointed to the role of chloride (Schnermann et al. 1976). On account of these observations it has been suggested that in pathological conditions a defective absorption of NaCl by damaged proximal tubule cells might act as a negative feed-back on the GFR (Bohle and Thurau 1974), which could explain the funtional shut-down associated with acute renal failure. As demonstrated in this study proximal tubule atrophy includes a reduction of the basolateral membranes and the mitochondria, which are generally considered to mediate the active transport of sodium and secondarily passive transport of chloride. Hence, it is possible that proximal tubule atrophy also in supposedly early stages may exert a negative feed-back effect on the GFR with the ensuing risk of prepetuating the tubular damage. In this connection it is noteworthy that in recent ultrastructural analyses of proximal tubule changes in acute renal failure one of the main changes of proximal tubule cells appeared to be a reduction of the basolateral membranes (Jones 1982; Olsen and Olsen 1983).

References

Anderson MS (1963) Electron microscopy of the glomerulus and renal tubules in experimental hypertension. Am J Pathol 43:257–272

Barka T, Anderson PJ (1962) Histochemical methods for acid phosphatase using hexazonium pararosanilin as coupler. J Histochem Cytochem 10:741–753

Benitez L, Shaka JA (1964) Cell proliferation in experimental hydronephrosis and compensatory renal hyperplasia. Am J Pathol 44:961–972

Berger SJ, Sacktor B (1970) Isolation and histochemical characterization of brush borders from rabbit kidney. J Cell Biol 47:637–645

Bernard BD, Thomasson D, Zenser TV (1983) Renal disease profoundly alters cortical interstitial cell function. Kidney Int 23:458–464

Bohle A, Thurau K (1974) Funktion und Morphologie der Niere im akuten Nierenversagen. Verhandl Deutsch Gesellsch Inn Med 80:565–582

Bohle A, Grund KE, Mackensen S, Tolon M (1977a) Correlations between renal interstitium and level of serum creatinine. Morphometric investigations of biopsies in perimembranous glomerulonephritis. Virchows Arch [Pathol Anat] 373:15–22

Bohle A, Bader R, Grund KE, Mackensen S, Neunhoeffer J (1977b) Serum creatinine concentration and renal interstitial volume. Analysis of correlations in endocapillary (acute) glomerulonephritis and in moderately severe mesangioproliferative glomerulonephritis. Virchows Arch [Pathol Anat] 375:87–96

Bohman S-O (1983) The ultrastructure of the renal interstitium. In: Cotran RS, Brenner BM, Stein JH (eds) Tubulo-interstitial nephropathies. Churchill Livingstone, New York, pp 1–34

Chatelanat F, Simon GT (1969) Ultrastructural pathology of the tubules and interstitial tissue. In: Rouiller C and Muller AF (eds) The kidney, vol. 1, Academic Press, New York, pp 449–530

Christensen EI, Madsen KM (1978) Renal age changes. Observations on the rat kidney cortex with special reference to structure and function of the lysosomal system in the proximal tubule. Lab Invest 39:289–297

Christensen EI, Maunsbach AB (1980) Proteinuria induced by sodium maleate in rats: Effects on ultrastructure and protein handling in renal proximal tubule. Kidney Int 17:771–787

Christensen EI, Maunsbach AB, Lüllmann-Rauch R (1983) Renal lysosomal protein digestion in experimental lipidosis. Virchows Arch [Cell Pathol] 43:309–316

Clark SL (1957) Cellular differentiation in the kidneys of newborn mice studied with the electron microscope. J Biophys Biochem Cytol 3:349–362

Cuppage FE, Tate A (1967) Repair of the nephron following injury with mercuric chloride. Am J Pathol 51:405–429

David H (1963) Submikroskopische Strukturveränderungen der Niere bei akuter und subakuter Harnstauung (Hydronephrose). Acta Biol Med Germ 10:164–173

David H, Uerlings I (1964) Die Wirkung der Äthylenglykolvergiftung auf das submikroskopische Bild der Rattenniere. Acta Biol Med Germ 12:203–218

Dobyan DC, Nagle RB, Bulger RE (1977) Acute tubular necrosis in the rat kidney following sustained hypotension. Physiologic and morphologic observations. Lab Invest 37:411–422

Dobyan DC, Cronin RE, Bulger RE (1982) Effect of potassium depletion on tubular morphology in gentamicin-induced acute renal failure in dogs. Lab Invest 47:586–594

Ericsson JLE, Bergstrand A, Andres G, Bucht H, Cinotti G (1965) Morphology of the renal tubular epithelium in young healthy humans. Acta Pathol Microbiol Scand 63:361–384

Ericsson JLE, Andres G, Bergstrand A, Bucht H, Orsten P-Å (1967) Further studies on the fine structure of renal tubules in healthy humans. Acta Pathol Microbiol Scand 69:493–513

Farquhar MG, Vernier RL, Good RA (1957) The application of electron microscopy in pathology: Study of renal biopsy tissues. Schweiz Med Wochenschr 17:501–510

Flume JB, Ashworth CT, James JA (1963) An electron microscopic study of tubular lesions in human kidney biopsy specimens. Am J Pathol 43:1067–1087

Giebisch G (1978) The proximal nephron. In: Andreoli TE, Hoffman JF (eds) Physiology of membrane disorders. Plenum Publishing Corporation, pp 629–660

Gise Hv, Gise Vv, Stark B, Bohle A (1981) Nephrotic syndrome and renal insufficiency in association with amyloidosis: A correlation between structure and function. Klin Wochenschr 59:75–82

Glaumann B, Glaumann H, Berezesky IK, Trump BF (1975) Studies on the pathogenesis of ischemic cell injury. II. Morphological changes of the pars convoluta (P1 and P2) of the proximal tubule of the rat kidney made ischemic in vivo. Virchows Arch [Cell Pathol] 19:281–302

Glaumann B, Glaumann H, Berezesky IK, Trump BF (1977) Studies on cellular recovery from injury II. Ultrastructural studies on the recovery of the pars convoluta of the proximal tubule of the rat kidney from temporary ischemia. Virchows Arch [Cell Pathol] 24:1–18

Grund KE, Mackensen S, Grüner J, Neunhoeffer J, Bader H, Bohle A (1978) Renal insufficiency in nephrosclerosis (Benign nephrosclerosis resp. transition from benign to secondary

malignant nephrosclerosis). Correlation between morphologial and functional parameters. Klin Wochenschr 56:1147–1154
Houghton DC, Hartnett M, Champbell-Boswell M, Porter G, Bennett W (1976) A light and electron microscopic analysis of gentamicin nephrotoxicity in rats. Am J Pathol 82:589–612
Jepsen FL, Mortensen PB (1979) Interstitial fibrosis of the renal cortex in minimal change lesion and its correlation with renal function. A quantitative study. Virchows Arch [Pathol Anat] 383:265–270
Jones DB (1982) Ultrastructure of acute renal failure. Lab Invest 46:254–264
Kaissling B, Kriz W (1979) Structural analysis of the rabbit kidney. In: Brodal A, Hild W, Limborgh Jv, Ortmann R, Schibler TH, Töndury G, Wolff E (eds) Advances in anatomy, embryology and cell biology, vol. 56, Springer, Berlin Heidelberg New York
Katz AI (1982) Renal Na-K-ATPase: its role in tubular sodium and potassium transport. Am J Physiol 242:(renal fluid electrolyte physiol. 11), F207–F219
Kelly RE, Rice RV (1968) Localization of myosin filaments in smooth muscle. J Cell Biol 37:105–116
Kempczinski RF, Caulfield JB (1968) A light and electron microscopic study of renal tubular regeneration. Nephron 5:249–264
Larsson L (1975) The ultrastructure of the developing proximal tubule in the rat kidney. J Ultrastruct Res 51:119–139
Larsson L, Horster M (1976) Ultrastructure and net fluid transport in isolated perfused developing proximal tubules. J Ultrastruct Res 54:276–285
Latta H, Osvaldo L, Jackson JD, Cook ML (1965) Changes in renal cortical tubules during autolysis. Electron microscopic observations. Lab Invest 14:635–657
Mackensen S, Grund KE, Sindjić M, Bohle A (1979) Influence of the renal cortical interstitium on the serum creatinine concentration and serum creatinine clearence in different chronic sclerosing interstitial nephritides. Nephron 24:30–34
Mackensen-Haen S, Bader R, Grund KE, Bohle A (1981) Correlations between renal cortical interstitial fibrosis, atrophy of the proximal tubules and impairment of the glomerular filtration rate. Clin Nephrol 15:167–171
Maunsbach AB, Madden SC, Latta H (1962) Variations in fine structure of renal tubular epithelium under different conditions of fixation. J Ultrastruct Res 6:511–530
Maunsbach AB (1966a) Absorption of I^{125}-labeled homologous albumin by rat kidney proximal tubule cells. A study of microperfused single proximal tubules by electron microscopic autoradiography and histochemistry. J Ultrastruct Res 15:197–241
Maunsbach AB (1966b) Observations on the ultrastructure and acid phosphatase activity of the cytoplasmic bodies in rat kidney proximal tubule cells. With a comment on their classification. J Ultrastruct Res 16:197–238
Maunsbach AB (1973) Ultrastructure of the proximal tubule. In: Orloff J, Berliner RW (eds) Handbook of Physiology, sect 8 Renal Physiology, American Physiological Society, Washington DC, pp 31–79
Maunsbach AB (1979) The tubule. In: Johannessen JV (ed) Electron microscopy in human medicine, vol 9, McGraw-Hill, New York, pp 143–165
Mergner WJ, Chang SH, Trump BF (1976) Studies on the pathogenesis of ischemic cell injury. Morphologic changes of the pars convoluta (P1 and P2) of the proximal tubule of rat kidney made ischemic in vitro. Virchows Arch [Cell Pathol] 21:211–228
Myler RK, Lee JC, Hopper J (1964) Renal tubular necrosis caused by mushroom poisoning. Arch Int Med 114:196–204
Møller JC, Skriver E, Olsen S, Maunsbach AB (1982) Perfusion-fixation of human kidneys for ultrastructural analysis. Ultrastruct Pathol 3:375–385
Nagle RB, Bulger RE, Cutler RE, Jervis HR, Benditt EP (1973a) Unilateral obstructive nephropathy in the rabbit. I. Early morphologic, physiologic, and histochemical changes. Lab Invest 28:456–467
Nagle RB, Kneiser MR, Bulger RE, Benditt EP (1973b) Induction of smooth muscle characteristics in renal interstitial fibroblasts during obstructive nephropathy. Lab Invest 29:422–427
Nagle RB, Johnson ME, Jervis HR (1976) Proliferation of renal interstitial cells following injury induced by ureteral obstruction. Lab Invest 35:18–22

Olsen TS and Olsen HS (1983) A second look on renal ultrastructure in acute renal failure. In: Solez K, Whelton A (eds) Acute renal failure, Dekker, New York (in press)
Ormos J, Solbach H-G (1963) Beitrag zur Morphologie der Niere bei Diabetes mellitus. Frankfurter Z Pathol 72:379–418
Ormos J, Elemér G, Csapó Z (1973) Ultrastructure of the proximal convoluted tubules during repair following hormonally induced necrosis in rat kidney. Virchows Arch B Zellpath 13:1–13
Pease DC (1968) Myoid features of renal corpuscles and tubules. J Ultrastruct Res 23:304–320
Pedersen JC, Persson AEG, Maunsbach AB (1980) Ultrastructure and quantitative characterization of the cortical interstitium in the rat kidney. In: Maunsbach AB, Olsen TS, Christensen EI (eds) The functional ultrastructure of the kidney. Academic Press Inc, London, pp 443–456
Reimer KA, Ganote CE, Jennings RB (1972) Alterations in renal cortex following ischemic injury. III. Ultrastructure of proximal tubules afer ischemia or autolysis. Lab Invest 26:347–363
Riemenschneider T, Mackensen-Haen S, Christ H, Bohle A (1980) Correlation between endogenous creatinine clearence and relative interstitial volume of the renal cortex in patients with diffuse membranous glomerulonephritis having a normal serum creatinine concentration. Lab Invest 43:145–149
Risdon RA, Sloper JC, de Wardener HE (1968) Relationship between renal function and histological changes found in renal-biopsy specimens from patients with persistent glomerular nephritis. Lancet II:363–366
Romen W, Mäder-Kruse I (1978) The basement membrane of the atrophic kidney tubule. An electron microscopic study of changes in rats. Virchows Arch [Cell Pathol] 26:307–319
Rostgaard J, Kristensen BI, Nielsen LE (1972) Electron microscopy of filaments in the basal part of rat kidney tubule cells and their in situ interaction with heavy meromyosin. Z Zellforsch 132:497–521
Schainuck LI, Striker GE, Cutler RE, Benditt EP (1970) Structural-functional correlations in renal disease. II: The correlations. Hum Pathol 1:631–641
Schnermann J, Ploth DW, Hermle M (1976) Activation of tubulo-glomerular feedback by chloride transport. Pflügers Arch 362:229–240
Shimamura T, Kissane JM, Györkey F (1966) Experimental hydronephrosis. Nephron dissection and electron microscopy of the kidney following obstruction of the ureter and in recovery from obstruction. Lab Invest 15:629–640
Sloper JC, de Wardener H, Woodrow DF (1980) Relationship between renal structure and function deduced from renal biopsies. In: Leaf A, Giebisch G, Bolis L, Gorini S (eds) Renal Pathophysiology, Raven Press, New York, pp 109–120
Suzuki T, Furusato M, Takasaki S, Ishikawa E (1975) Giant mitochondria in the epithelial cells of the proximal convoluted tubules of diseased human kidneys. Lab Invest 33:578–590
Thoenes W (1966) Über matrixreiche Riesenmitochondrien. Elektronenmikroskopische Beobachtungen am Tubulusepithel der menschlichen Niere bei nephrotischem Syndrom. Z Zellforsch 75:422–433
Thurau K, Schnermann J (1965) Die Natriumkonzentration an den Macula densa-Zellen als regulierender Faktor für das Glomerulumfiltrat (Mikropunktionsversuche). Klin Wochenschr 43:410–413
Thurau K, Dörge A, Rick R, Bauer R, Beck F, Mason J, Roloff C (1980) Quantification of intracellular elements in frog skin and tubular cells under different functional conditions by means of electron microprobe analysis. In: Maunsbach A, Olsen TS, Christensen EI (eds) Functional ultrasturcture of the kidney, Academic Press, London, pp 177–190
Tisher CC, Bulger RE, Trump BF (1966) Human renal ultrastructure. I. Proximal tubule of healthy individuals. Lab Invest 15:1357–1394
Tisher CC, Rosen S, Osborne GB (1969) Ultrastructure of the proximal tubule of the rhesus monkey kidney. Am J Pathol 56:469–517
Venkatachalam MA, Bernard DB, Donohoe JF, Levinsky NG (1978) Ischemic damage and repair in the rat proximal tubule: Differences among the S1, S2 and S3 segments. Kidney Int 14:31–49

Verani RR, Brewer ED, Ince A, Gibson J, Bulger RE (1982) Proximal tubular necrosis associated with maleic acid administration to the rat. Lab Invest 46:79–88

Wellwood JM Lovell D, Thompson AE, Tighe JR (1975) Renal damage caused by gentamicin: A study of the effects on renal morphology and urinary enzyme excretion. J Pathol 118:171–182

Wilson DR (1980) Pathophysiology of obstructive nephropathy. Kidney Int 18:281–292

Wright FS, Briggs JP (1979) Feedback control of glomerular blood flow, pressure, and filtration rate. Phys Rev 59:958–1006

Zollinger HU, Torhorst J, Riede UN, Toenges Vv, Geering B, Rohr H-P (1973) Der inkomplette oder Sub-infarkt der Niere (einseitig zentral-arterielle Schrumpfniere). Pathologisch-anatomische, morphometrische und elektronenmikroskopische Untersuchungen. Beitr Pathol 148:15–34

Accepted September 7, 1983